MOX-Report No. 08/2019

Computational analysis of turbulent haemodynamics in radiocephalic arteriovenous fistulas with different anastomotic angles

Prouse, G.; Stella, S.; Vergara, C.; Engelberger, S.; Trunfio, R.;

Canevascini, R.; Quarteroni, A.; Giovannacci, L.

MOX, Dipartimento di Matematica
Politecnico di Milano, Via Bonardi 9 - 20133 Milano (Italy)

mox-dmat@polimi.it http://mox.polimi.it

COMPUTATIONAL ANALYSIS OF TURBULENT HAEMODYNAMICS IN RADIOCEPHALIC ARTERIOVENOUS FISTULAS WITH DIFFERENT ANASTOMOTIC ANGLES

Prouse G.[1], Stella S.[2], Vergara C.[2], Engelberger S.[1], Trunfio R.[1], Canevascini R.[1], Quarteroni A.[2], Giovannacci L.[1]

[1] Division of Visceral and Vascular Surgery, Lugano Regional Hospital, Lugano, Switzerland
[2] MOX Polytechnic of Milan, Department of Mathematics

ABSTRACT

Objective: Hemodynamics has been known to play a major role in the development of intimal hyperplasia (IH) leading to arteriovenous fistula failure. The goal of our study is to investigate the influence of different angles of side-to-end radiocephalic anastomosis upon the hemodynamic parameters that promote intimal dysfunction and therefore IH.

Methods: Realistic 3D meshes were reconstructed using ultrasound measurements from distal side-to-end radiocephalic fistulas. The velocity at the proximal and distal radial inflows and at specific locations along the anastomosis and cephalic vein was measured through single examiner duplex ultrasound. A computational parametric study, virtually changing the inner angle of anastomosis, was performed. For this purpose we used advanced computational models that include suitable tools to capture the pulsatile and turbulent nature of the blood flow found in arteriovenous fistulas. The results were analysed in terms of velocity fields, wall shear stress distribution and oscillatory shear index (OSI).

Results: Results show that the regions with high OSI, that are more prone to the development of hyperplasia, are greater and progressively shift toward the anastomosis area and the proximal vein segment with the decrease of the inner angle of anastomosis.

Conclusions: The results of this study show that inner anastomosis angles approaching 60°-70° seem to yield the best hemodynamic conditions for maturation and long term patency of distal radiocephalic fistulas. Inner angles greater than 90°, representing the smooth loop technique, did not show a clear hemodynamic advantage.

INTRODUCTION

Native vessel arteriovenous fistulas (AVFs) are currently considered the best choice for a vascular access in haemodialysis patients [1]. The radiocephalic side-to-end forearm fistula is often used as a first access in patients with suitable vessels but it is burdened by a high rate of maturation failure which ranges between 20 and 50 % in recent series [1/2/3/4/5]. One of the known mechanisms for this primary failure is early intimal hyperplasia (IH). Late failure, defined as the inability to use a maturated AVF after at least three months of normal usage, relies mainly on the presence of stenosis from intimal hyperplasia at different possible segments of the vessels. Haemodynamics has been recognized to play an important role in the development of IH [6/7/8], with areas of disturbed flow creating the conditions that favor endothelial dysfunction and the development of vessel stenosis [9/10]. Computational models

are an effective tool to study the complexity of disturbed flows in a non-invasive manner, allowing the analysis of the local haemodynamic factors that are involved in the risk of early and late failure of AVFs [11,12,13]. The goal of this work is to perform a computational study on three-dimensional geometries reconstructed from measurements of radiocephalic AVFs from 2 different patients, comparing the disturbed haemodynamics in different anastomotic angles.

MATERIALS AND METHODS

The geometries of radiocephalic fistulas from two patients were reconstructed using data obtained from duplex ultrasound examinations performed by the same physician at 4 weeks from surgery. The patients were consecutive and received radiocephalic side-to-end fistulas fashioned by two different surgeons at the same centre (Ospedale Regionale di Lugano, Lugano, Switzerland). Patients gave written consent for the inclusion in the study which was approved by the regional ethics board. The inner anastomotic angles were 40° for patient 1 and 70° for patient 2. Both AVFs had proximal and distal radial artery inflow. The flow rate and velocity measurements obtained by duplex ultrasound at the proximal and distal radial inflow and at the cephalic vein outflow were utilised.

3D reconstructions were created using detailed duplex ultrasound measurements of diameters at multiple arterial and venous locations, of anastomosis angles and of geometric dispositions of the feeding and outflowing vessels. The anastomotic angles measured by ultrasound were compared to those measured intraoperatively by the surgeon and varied by no more than ± 10°. The lumen surface boundaries were reconstructed for the two AVFs in their original angles of 40° in patient 1 and 70° in patient 2, followed by the same procedure with modified angles. We chose additional acute angles of 20° and 60° for patient 1 and of 30° and 50° for patient 2. Furthermore, an angle of 135° was reconstructed for both patients reproducing the geometry of a smooth loop anastomosis technique proposed by some authors [14/15]. The reconstruction of the internal volume in the different angles and geometries was then performed through volumetric meshes of linear tetrahedra with sufficient resolution for our study (Fig. 1).

Blood was considered an incompressible Newtonian fluid with constant density, which is a well- accepted approximation for medium and large vessels [16]. Turbulence was captured using advanced models (Large Eddy Simulations) [17/18/19/20], which have previously been successfully applied to haemodynamics [21/22]. A computational haemodynamic study with pulsatile inflow conditions was then performed for all 8 configurations obtaining the quantities of interest which are: the velocity distribution throughout the cardiac cycle, the wall shear stress (WSS), with low values promoting endothelial dysfunction, and the Oscillatory Shear Index (OSI) which identifies conditions of low shear stress with oscillating characteristics [23].

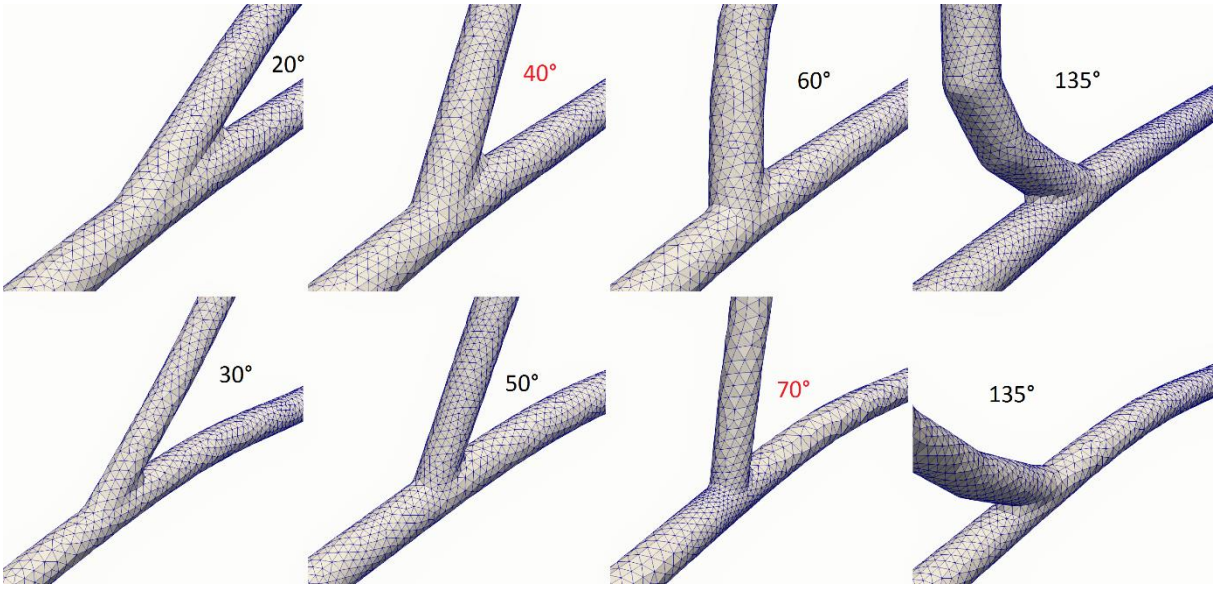

Figure 1 : Computational meshes of 4 different configurations of the AVFs in patient 1 (above) and patient 2 (below) with various anastomotic angles (patient 1 : 20°, 40°, 60°, 135° smooth loop, patient 2 : 30°, 50°, 70°, 135° smooth loop). In red: measured (original) angles

RESULTS

Our computational study identified some significant differences in relevant haemodynamic quantities when the inner angle of the AVF anastomosis was changed.
Figure 2 illustrates the velocities at different moments of the cardiac cycle. Increases of the inner angle were associated with greater velocities at the anastomosis in both patients.
Figure 3 depicts the evolution of wall shear stress over time for the three acute angles in three points on the vessel wall surface that have been set at critical peri-anastomotic sampling positions, namely at the anastomosis toe (central plots), 1 cm from the anastomosis along the external wall of the swing segment of the vein (plots on the left) and 1 cm from the anastomosis on the external wall of the distal radial artery (plots on the right). The plots show high WSS on the venous wall for all acute angles in patient 1, whereas in patient 2 the WSS is significantly lower in this segment for the smaller angle (30°). At the anastomosis site the WSS plots show remarkably higher values for the wider acute angles in both patients. At the distal radial artery the WSS values are significantly lower and these values decrease with smaller angles of incidence.
In order to integrate the data about the WSS with information about it's oscillatory nature we analyzed the spatial distribution of OSI. High values of this index are known to identify areas prone to developing IH. Figure 4 shows that for greater acute angles, the areas with high values of OSI gradually shift away from the anastomosis and toward the distal segment of the radial artery. This tendency is inverted for angles approaching 135°, which show an intermediate behavior with high OSI values approaching the anastomosis again. Similarly, as depicted in Table 1, the percentage of vessel wall area that is subjected to OSI values greater than specific thresholds decreases with greater acute angles. This is shown to be independent from the chosen threshold. The relative area with above threshold OSI values in the 135° configuration features intermediate results between small (20°-40°) and wide (60°-70°) acute angles. These results are specific to radiocephalic AVFs with proximal and distal radial inflow.

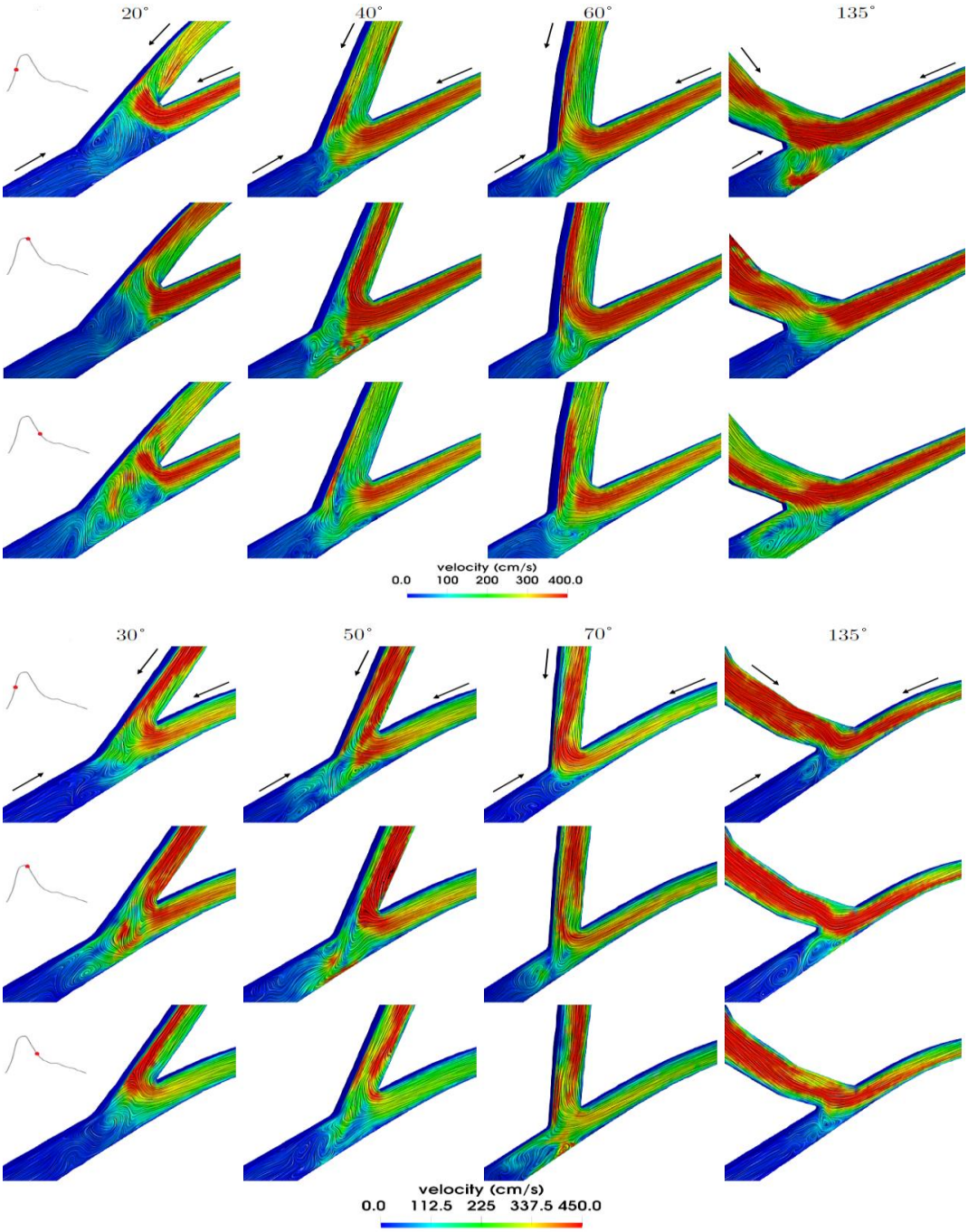

Figure 2 : Velocity for the different angle configurations of patient 1 (above) and patient 2 (below), at 3 different moments in the cardiac cycle: Acceleration instant t=0.12s; Peak t=0.21s; Mid-deceleration t=0.3s. The arrows during the acceleration-phase plots depict the dominant direction of flow.

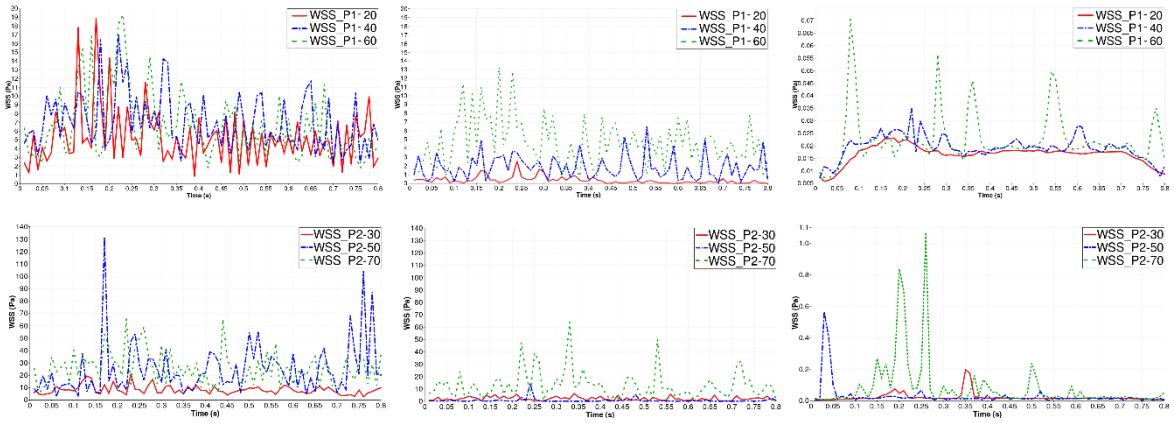

Figure 3 : Wall Shear Stress over time at the three selected points : cephalic vein 1 cm from anastomosis (left), anastomosis toe (center), distal radial artery 1 cm from anastomosis (right). Notice the different scale in plots on the right. Above : patient 1. Bottom : patient 2.

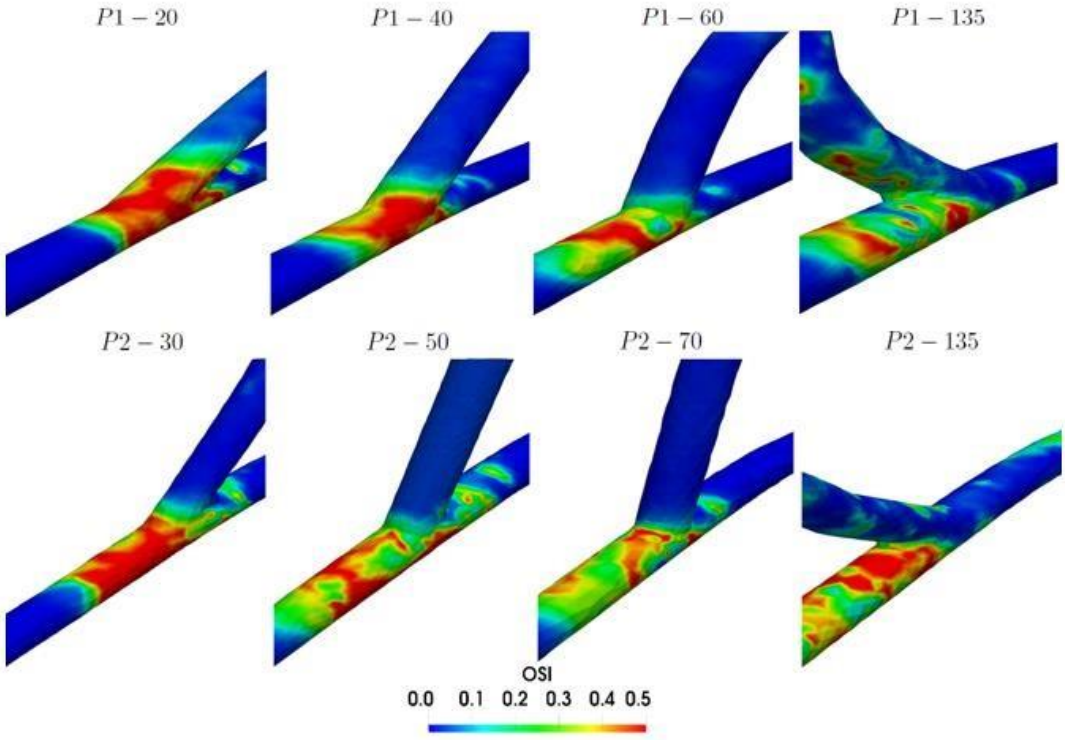

Figure 4 : Oscillatory Shear Index (OSI) in the area of anastomosis for patient 1 (top) and patient 2 (bottom).

Threshold/Angle	20°/30°	40°/50°	60°/70°	135°/135°
0.15	28.4/39.1%	21.3/25.8%	18.6/21.6%	25.3/29.4%
0.20	21.7/32.5%	15.2/19.8%	12.7/14.1%	17.9/22.6%
0.25	18.2/28.8%	13.3/17.5%	9.9/12.2%	14.1/20.3%

Table 1: Proportion of vessel wall surface in the region of interest with Oscillatory Shear Index (OSI) above a specific threshold. For each box, on the left patient 1, on the right patient 2.

DISCUSSION

In the last 2 decades computational fluid dynamics have been successfully used to study the complex haemodynamics of AVFs and to assess the role of wall shear stress and its oscillation in the pathogenesis of IH [13]. There is, in fact, consensus in literature that low and oscillating values of wall shear stress cause endothelial dysfunction, hence atherosclerosis [9/10] and IH [24/25/26]. These critical flow characteristics are well described by high values of OSI [9/23].
Following this hypothesis, this study demonstrates that increases in the acute angle of anastomosis in both patients are associated with a reduced exposure to haemodynamic conditions that favor IH. Table 1 shows a smaller percentage of wall surface with OSI values above specific thresholds when greater acute angles of anastomosis are considered. This tendency is independent from the threshold chosen for critical OSI values. Also, the areas with high values of OSI move away from the anastomosis toward the distal segment of the radial artery with greater acute angles (Fig. 4). Although some authors describe an underestimation of inflow stenosis as the underlying cause for AFV failure [27/28], stenosis of the distal segment of the radial artery remains, in our experience, a rare cause for radiocephalic fistula failure.
The previous observations on OSI are confirmed by the velocity fields reported in Figure 2, which feature large vortices and stagnation regions at the anastomosis for small acute angles, yielding regions of low wall shear stress as shown in Figure 3. Greater acute angles, on the other hand, seem to facilitate a more aligned flow.

Some authors proposed the smooth loop technique [14/15] as a valid alternative to acute angle anastomoses typically performed in AVFs. To analyze the haemodynamics of this configuration an angle of 135° was introduced in our computational study for both patients. As depicted in Figure 4, for this scenario the area with high OSI values tends to move back towards the anastomosis. Similarly, Table 1 shows intermediate percentage of wall surface with high OSI values in the 135° configuration. When considering the velocity fields on the other hand, we found a comparable situation in the smooth loop anastomosis as in the wider acute angles (Fig. 2). Hence, these preliminary results concerning the smooth loop anastomosis do not show a

clear advantage of this technique over the greater acute angle anastomoses. However, further investigations are needed to properly evaluate this technique analyzing, for example, different angles of incidence.

In recent years several numerical studies have been performed to attempt to assess the risk of failure of AVFs. The first parametric study evaluating the size and the angle of AVF anastomosis was published by Canneyt et al. in 2010 [13]. This pioneering analysis assumed rigid vessel walls and steady laminar flow. Numerical simulations were performed, with the aim of determining the changes in flow distribution and in pressure drop with the variation of anastomosis angle and area. More recently, some investigators published a similar study, but introduced pulsatile inflow conditions and evaluated wall shear stress derived quantities to assess the clinical impact of different anastomosis angles [29]. Supplemental to the approaches used in these two studies, we used here patient-specific instead of idealized geometries and introduced a turbulence model in pulsatile conditions.

The findings in this study suggest that the best haemodynamic conditions, in terms of risk of IH in the anastomosis and in the first segment of the cephalic vein, are offered by inner angles close to 60°-70°. These angles of anastomosis, compared to angles of 20°-30°, may pose a technical challenge when attempting to establish a large enough anastomosis surface with a small vein (Fig. 5). Several different side-to-end anastomosis techniques have been described in the literature, some of which could be useful to overcome this difficulty. In our experience a venous branch-patch [30] (Fig. 6) offers a good opportunity to construct a wide angle anastomosis with a smooth bell-bottom shaped venous extremity. Unfortunately, an adequately positioned venous bifurcation is not always available. Some authors report this technique to potentially increase torsion stress on the swing-segment of the vein leading to IH [31]. For this reason, the branch-patch technique should be chosen only when the available bifurcation lays in an adequate plane to be used for the anastomosis. As an alternative, when an adequate venous branch is not available, Williams et al. proposed a vein mouth technique [32] (Fig. 7). The downside of this technique is that the suture runs through the two commissures of the venotomy, potentially inducing hyperplasia in the most narrow passage into the vein. Another technique, that has been proposed by Sen et al. in his microsurgical work and successfully adopted by some authors for side-to-end AVF anastomosis [33], uses a diamond shaped hole arteriotomy with correspondingly shaped vein, as illustrated in Figure 8. The authors report being able to successfully adapt the arteriotomy and venotomy to accommodate different anastomotic angles. These different techniques all have their strengths and weaknesses and are not applicable to all anatomies. We believe that the surgeon should ideally master more than one technique in order to be able to create the desired geometry with an adequate anastomotic angle in the different anatomic settings he is faced with.

Figure 5: Venotomies and anastomosis size at different angle

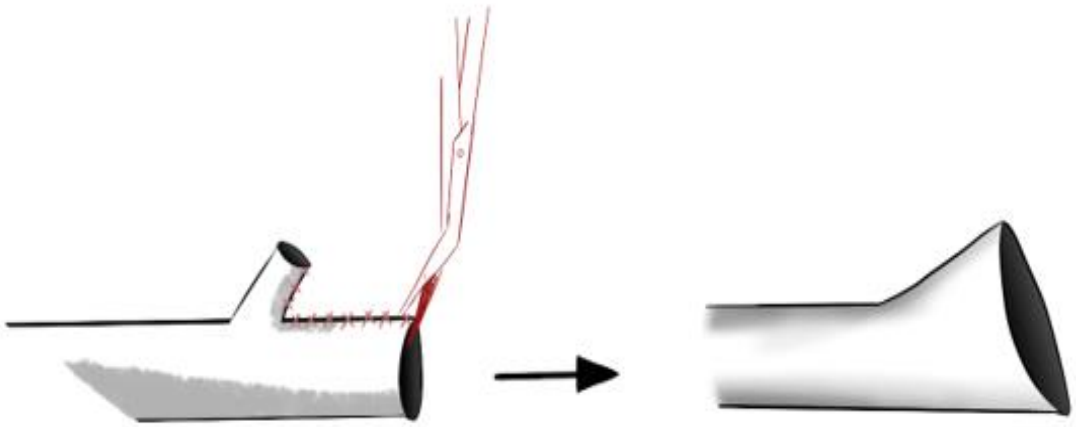

Figure 6: Venous branch-patch technique

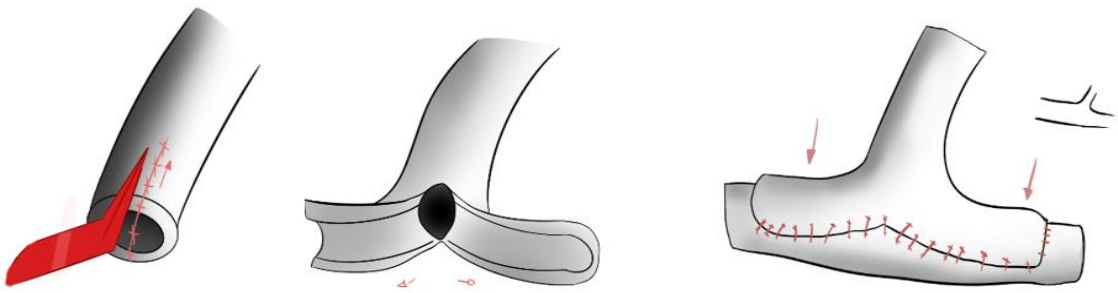

Figure 7: Vein mouth technique

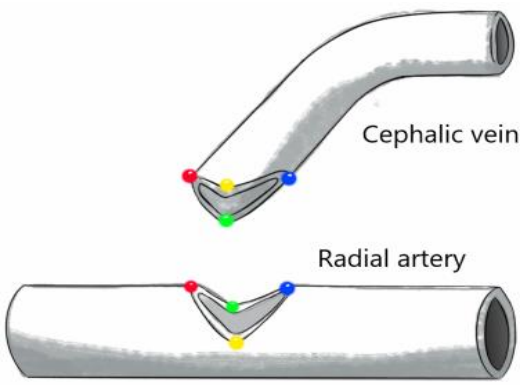

Figure 8: Diamond shaped anastomosis technique

CONCLUSIONS

Although intimal hyperplasia developing in proximity to the anastomosis and in the first venous segment may have several underlying causes, haemodynamic factors are recognized to play an important role. The results of this computational haemodynamic study demonstrate that inner anastomotic angles of 60°-70° seem to yield the best conditions for maturation and long term patency of distal radiocephalic fistulas. This geometry reduces the vessel wall area subjected to high oscillating shear index in the anastomosis and in the first vein segment. Anastomotic angles greater than 90° did not show a clear advantage although a dedicated study for this configuration is needed to confirm these findings.

FUNDING

This study was internally funded by the Scientific Research Advisory Board of our institution (ABREOC)

CONFLICT OF INTEREST

None.

REFERENCES :

1. Kalman PG, Pope M, Bhola C, Richardson R, Sniderman KW. A practical approach to

vascular access for hemodialysis and predictors of success. *J Vasc Surg*. 1999. doi:10.1016/S0741-5214(99)70112-6
2. Ernandez T, Saudan P, Berney T, Merminod T, Bednarkiewicz M, Martin PY. Risk factors for early failure of native arteriovenous fistulas. *Nephron - Clin Pract*. 2005. doi:10.1159/000085710
3. Patel ST, Hughes J, Mills JL, Huber TS. Failure of arteriovenous fistula maturation: An unintended consequence of exceeding Dialysis Outcome Quality Initiative guidelines for hemodialysis access. *J Vasc Surg*. 2003. doi:10.1016/S0741-5214(03)00732-8
4. Lok CE, Allon M, Moist L, Oliver MJ, Shah H, Zimmerman D. Risk Equation Determining Unsuccessful Cannulation Events and Failure to Maturation in Arteriovenous Fistulas (REDUCE FTM I). *J Am Soc Nephrol*. 2006. doi:10.1681/ASN.2006030190
5. Allon M, Robbin ML. Increasing arteriovenous fistulas in hemodialysis patients: Problems and solutions. *Kidney Int*. 2002. doi:10.1046/j.1523-1755.2002.00551.x
6. Hofstra L, Bergmans DC, Leunissen KM, Hoeks AP, Kitslaar PJ, Tordoir JH. Prosthetic arteriovenous fistulas and venous anastomotic stenosis: influence of a high flow velocity on the development of intimal hyperplasia. *Blood Purif*. 1996.
7. Corpataux J-M. Low-pressure environment and remodelling of the forearm vein in Brescia-Cimino haemodialysis access. *Nephrol Dial Transplant*. 2002. doi:10.1093/ndt/17.6.1057
8. He Y, Terry CM, Nguyen C, Berceli SA, Shiu YTE, Cheung AK. Serial analysis of lumen geometry and hemodynamics in human arteriovenous fistula for hemodialysis using magnetic resonance imaging and computational fluid dynamics. *J Biomech*. 2013. doi:10.1016/j.jbiomech.2012.09.005
9. Ku DN, Giddens DP, Zarins CK, Glagov S. Pulsatile flow and atherosclerosis in the human carotid bifurcation. Positive correlation between plaque location and low oscillating shear stress. *Arterioscler Thromb Vasc Biol*. 1985. doi:10.1161/01.ATV.5.3.293
10. Malek AM, Alper SL, Izumo S. Hemodynamic shear stress and its role in atherosclerosis. *J Am Med Assoc*. 1999. doi:10.1001/jama.282.21.2035
11. Ene-Iordache B, Mosconi L, Cele Daccò A, Negri M, Remuzzi G, Remuzzi A. Computational Fluid Dynamics of a Vascular Access Case for Hemodialysis. *J Biomech Eng*. 2001. doi:10.1115/1.1372702
12. Kharboutly Z, Fenech M, Treutenaere JM, Claude I, Legallais C. Investigations into the relationship between hemodynamics and vascular alterations in an established arteriovenous fistula. *Med Eng Phys*. 2007. doi:10.1016/j.medengphy.2006.10.018
13. Van Canneyt K, Pourchez T, Eloot S, et al. Hemodynamic impact of anastomosis size and angle in side-to-end arteriovenous fistulae: A computer analysis. *J Vasc Access*. 2010. doi:10.1177/112972981001100111
14. Karmody AM, Lempert N. “Smooth loop” arteriovenous fistulas for hemodialysis. *Surgery*. 1973.
15. Ansari MM, Viridi JS, Hanif Beg M, Reyazuddin, Haleem S. Smooth Venous Loop Arterio Venous Fistula for Hemodialysis. *Vasc Endovascular Surg*. 1991. doi:10.1177/153857449102500708
16. Formaggia L, Quarteroni a, Veneziani a. *Cardiovascular Mathematics: Modeling and Simulation of the Circulatory System*.; 2009. doi:10.1007/978-88-470-1152-6
17. Nicoud F, Toda HB, Cabrit O, Bose S, Lee J. Using singular values to build a subgrid-scale model for large eddy simulations. *Phys Fluids*. 2011. doi:10.1063/1.3623274
18. Rogallo RS. Effect of rotation on isotropic turbulence: Computation and modelling. *J Fluid Mech*. 1985. doi:10.1017/S0022112085001550

19. Sturm M, Lee H, Thomas S, Barber T. The haemodynamic effect of an adjustable band in an arteriovenous fistula. *Comput Methods Biomech Biomed Engin*. 2017. doi:10.1080/10255842.2017.1315635
20. Broderick SP, Houston JG, Walsh MT. The influence of the instabilities in modelling arteriovenous junction haemodynamics. *J Biomech*. 2015. doi:10.1016/j.jbiomech.2015.07.038
21. Vergara C, Le Van D, Quadrio M, Domanin M. Large eddy simulations of blood dynamics in abdominal aortic aneurysms. *Med Eng Phys*. 2017. doi:10.1016/j.medengphy.2017.06.030
22. Lancellotti RM, Vergara C, Valdettaro L, Bose S, Quarteroni A. Large eddy simulations for blood dynamics in realistic stenotic carotids. *Int j numer method biomed eng*. 2017. doi:10.1002/cnm.2868
23. Lee S-W, Antiga L, Steinman DA. Correlations Among Indicators of Disturbed Flow at the Normal Carotid Bifurcation. *J Biomech Eng*. 2009. doi:10.1115/1.3127252
24. Lemson MS, Daemen MJAP, Kitslaar PJEHM, Tordoir JHM. A new animal model to study intimal hyperplasia in arteriovenous fistulas. *J Surg Res*. 1999. doi:10.1006/jsre.1999.5566
25. Meirson T, Orion E, Di Mario C, et al. Flow patterns in externally stented saphenous vein grafts and development of intimal hyperplasia. *J Thorac Cardiovasc Surg*. 2015. doi:10.1016/j.jtcvs.2015.04.061
26. Ene-Iordache B, Remuzzi A. Disturbed flow in radial-cephalic arteriovenous fistulae for haemodialysis: Low and oscillating shear stress locates the sites of stenosis. *Nephrol Dial Transplant*. 2012. doi:10.1093/ndt/gfr342
27. Sivanesan S, How T V., Bakran A. Sites of stenosis in AV fistulae for haemodialysis access. *Nephrol Dial Transplant*. 1999. doi:10.1093/ndt/14.1.118
28. Asif A, Gadalean FN, Merrill D, et al. Inflow stenosis in arteriovenous fistulas and grafts: A multicenter, prospective study. *Kidney Int*. 2005. doi:10.1111/j.1523-1755.2005.00299.x
29. Ene-Iordache B, Cattaneo L, Dubini G, Remuzzi A. Effect of anastomosis angle on the localization of disturbed flow in "side-to-end" fistulae for haemodialysis access. *Nephrol Dial Transplant*. 2013. doi:10.1093/ndt/gfs298
30. Jennings WC, Kindred MG, Broughan TA. Creating Radiocephalic Arteriovenous Fistulas: Technical and Functional Success. *J Am Coll Surg*. 2009. doi:10.1016/j.jamcollsurg.2008.11.015
31. Bharat A, Jaenicke M, Shenoy S. A novel technique of vascular anastomosis to prevent juxta-anastomotic stenosis following arteriovenous fistula creation. *J Vasc Surg*. 2012. doi:10.1016/j.jvs.2011.07.090
32. Williams L, Patselas T. The "Vein Mouth," an Alternative to the Branch Patch Technique for Arteriovenous Anastomosis. *J Am Coll Surg*. 2009. doi:10.1016/j.jamcollsurg.2009.09.012
33. Kanko M, Sen C, Yavuz S, Unal C, Aksoy A, Berkı T. Evaluation of arteriovenous fistulas made with the diamond-shaped anastomosis technique. *Med Sci Monit*. 2012. doi:10.12659/MSM.883337

MOX Technical Reports, last issues

Dipartimento di Matematica
Politecnico di Milano, Via Bonardi 9 - 20133 Milano (Italy)

05/2019 Gasperoni, F.; Ieva, F.; Paganoni, A.M.; Jackson, C.; Sharples, L.
Evaluating the effect of healthcare providers on the clinical path of Heart Failure patients through a novel semi-Markov multi-state model

06/2019 Pagani, S.; Manzoni, A.; Carlberg, K.
Statistical closure modeling for reduced-order models of stationary systems by the ROMES method

07/2019 Dal Santo, N.; Manzoni, A.
Hyper-reduced order models for parametrized unsteady Navier-Stokes equations on domains with variable shape

04/2019 Delpopolo Carciopolo, L.; Formaggia, L.; Scotti, A.; Hajibeygi, H.
Conservative multirate multiscale simulation of multiphase flow in heterogeneous porous media

03/2019 Ratti, L.; Verani, M.
A posteriori error estimates for the monodomain model in cardiac electrophysiology

02/2019 Micheletti, S.; Perotto, S.; Soli, L.
Topology optimization driven by anisotropic mesh adaptation: towards a free-form design

01/2019 Regazzoni, F.; Dedè, L.; Quarteroni, A.
Machine learning for fast and reliable solution of time-dependent differential equations

64/2018 Menafoglio, A.; Pigoli, D.; Secchi, P.
Kriging Riemannian Data via Random Domain Decompositions

66/2018 Riccobelli, D.; Agosti, A.; Ciarletta, P.
On the existence of elastic minimizers for initially stressed materials

65/2018 Boschi, T.; Chiaromonte, F.; Secchi, P.; Li, B.
Covariance based low-dimensional registration for function-on-function regression